JPn Neuroscience
The Journal of Physiology

A role for loop G in the β1 strand in $GABA_A$ receptor activation

Daniel T. Baptista-Hon[1], Alexander Krah[2], Ulrich Zachariae[2] and Tim G. Hales[1]

[1] *The Institute of Academic Anaesthesia, Division of Neuroscience, School of Medicine, Ninewells Hospital, University of Dundee, Dundee, UK*
[2] *Computational Biology, School of Life Sciences, University of Dundee, Dundee, UK*

Key points

- The role of the β1 strand in $GABA_A$ receptor function is unclear. It lies anti-parallel to the β2 strand, which is known to participate in receptor activation.
- Molecular dynamics simulation revealed solvent accessible residues within the β1 strand of the $GABA_A$ β3 homopentamer that might be amenable to analysis using the substituted Cys accessibility method.
- Cys substitutions from Asp43 to Thr47 in the $GABA_A$ α1 subunit showed that D43C and T47C reduced the apparent potency of GABA. F45C caused a biphasic GABA concentration–response relationship and increased spontaneous gating.
- Cys43 and Cys47 were accessible to 2-aminoethyl methanethiosulphonate (MTSEA) modification, whereas Cys45 was not. Both GABA and the allosteric agonist propofol reduced MTSEA modification of Cys43 and Cys47.
- By contrast, modification of Cys64 in the β2 strand loop D was impeded by GABA but unaffected by propofol.
- These data reveal movement of β1 strand loop G residues during agonist activation of the $GABA_A$ receptor.

Abstract The $GABA_A$ receptor α subunit β1 strand runs anti-parallel to the β2 strand, which contains loop D, known to participate in receptor activation and agonist binding. However, a role for the β1 strand has yet to be established. We used molecular dynamics simulation to quantify the solvent accessible surface area (SASA) of β1 strand residues in the $GABA_A$ β3 homopentamer structure. Residues in the complementary interface equivalent to those between Asp43 and Thr47 in the α1 subunit have an alternating pattern of high and low SASA consistent with a β strand structure. We investigated the functional role of these β1 strand residues in the α1 subunit by individually replacing them with Cys residues. D43C and T47C substitutions reduced the apparent potency of GABA at $\alpha1\beta2\gamma2$ receptors by 50-fold and eight-fold, respectively, whereas the F45C substitution caused a biphasic GABA concentration–response relationship and increased spontaneous gating. Receptors with D43C or T47C substitutions were sensitive to 2-aminoethyl methanethiosulphonate (MTSEA) modification. However, GABA-evoked currents mediated by $\alpha1$(F45C)$\beta2\gamma2$ receptors were unaffected by MTSEA, suggesting that this residue is inaccessible. Both GABA and the allosteric agonist propofol reduced MTSEA modification of $\alpha1$(D43C)$\beta2\gamma2$ and $\alpha1$(T47C)$\beta2\gamma2$ receptors, indicating movement of the β1 strand even during allosteric activation. This is in contrast to $\alpha1$(F64C)$\beta2\gamma2$ receptors, where only GABA, but not propofol, reduced MTSEA modification. These findings provide the first functional evidence for movement of the β1 strand during gating of the receptor and identify residues that are critical for maintaining $GABA_A$ receptor function.

DOI: 10.1113/JP272463

(Resubmitted 6 April 2016; accepted after revision 9 May 2016; first published online 16 May 2016)
Corresponding author T. G. Hales: The Institute of Academic Anaesthesia, Division of Neuroscience, School of Medicine, Ninewells Hospital, University of Dundee, Dundee, DD1 9SY, UK. E-mail: t.g.hales@dundee.ac.uk

Abbreviations DMEM, Dulbecco's modified Eagle's medium; DTT, dithiothreitol; HEK-293, human embryonic kidney 293 cell; MD, molecular dynamics; MTS, methanethiosulphonate; MTSEA, 2-aminoethyl methanethiosulphonate; PhMTS, phenylmethanethiosulphonate; pLGIC, pentameric ligand-gated ion channel; PTX, picrotoxin; SASA, solvent accessible surface area; SCAM, substituted cysteine accessibility method; TM, transmembrane; τ_w, weighted tau; WT, wild-type.

Introduction

$GABA_A$ receptors are members of the Cys-loop family of pentameric ligand-gated ion channels (pLGICs). $GABA_A$ receptors are assembled from 19 different subunits. The most common synaptic $GABA_A$ receptor consists of $\alpha1$, $\beta2$ and $\gamma2$ subunits (Whiting *et al.* 1995).

$GABA_A$ receptors have a large extracellular domain, housing the orthosteric ligand-binding site, and four transmembrane (TM) domains (TM1–4), which contain binding sites for allosteric agonists and several non-competitive antagonists. TM2 lines the Cl^--selective channel pore. Similar to most pLGICs, $GABA_A$ receptors also have a large intracellular domain, mainly composed of the TM3–4 loop (Baptista-Hon *et al.* 2013).

The orthosteric binding site, located at the interface between adjacent subunits (Smith & Olsen, 1995; Cromer *et al.* 2002), is lined by residues within six non-continuous loops (A–F) that participate in binding (Boileau *et al.* 1999; Holden & Czajkowski, 2002; Wagner *et al.* 2004; Goldschen-Ohm *et al.* 2011; Tran *et al.* 2011) and gating (Boileau *et al.* 2002; Newell & Czajkowski, 2003; Venkatachalan & Czajkowski, 2008; Szczot *et al.* 2014). In $GABA_A$ receptors, the primary interface contributes loops A, B and C, from the β subunit, whereas the complimentary interface contributes loops D, E and F, from the α subunit. These loops are contained within an anti-parallel β sandwich structure, which makes up much of the N-terminal domain.

Several pLGIC structures have recently been solved, with some in the presence of agonists providing an insight into the architecture of the orthosteric binding site. A structural model of *Caenorhabditis elegans* GluCl implicates $\beta1$ strand Arg37 in glutamate binding (Hibbs & Gouaux, 2011). This led to the proposal of a seventh binding loop, termed loop G. However, the equivalent $\beta1$ strand residue in *Aplysia californica* GluCl (Leu79) is not involved in its binding to glutamate or other amino acid agonists including GABA, suggesting that a role for the $\beta1$ strand in agonist binding may be restricted to the *C. elegans* GluCl (Blarre *et al.* 2014). Interestingly, replacement of *A. californica* GluCl Leu79 by Arg resulted in the abolition of glutamate evoked currents, highlighting the importance of amino acids in the $\beta1$ strand to receptor function. A comparison of GluCl structures in presumed open and closed conformations reveals that the $\beta1$ and $\beta2$ strands, as well as the $\beta1$–$\beta2$ loop, move towards the TM2–3 loop during gating (Althoff *et al.* 2014). This movement appears to precede the structural rearrangement of the TM domains that allow channel opening (Calimet *et al.* 2013). A similar conformational change has also been described in the structure of a zebrafish glycine receptor derived by cryo-electron microscopy (Du *et al.* 2015).

Residues in the $\beta1$ strand of the recently solved $GABA_A$ $\beta3$ homopentamer structure are not implicated in binding its agonist, benzamidine (Miller & Aricescu, 2014). However, residues in loop D of the anti-parallel $\beta2$ strand are involved, and this region of the $\alpha1$ subunit lies within the GABA binding pocket in $\alpha1\beta2\gamma2$ $GABA_A$ receptors (Boileau *et al.* 1999; Holden & Czajkowski, 2002). Furthermore, the loop D residue Phe64 participates in gating (Szczot *et al.* 2014). The use of the substituted Cys accessibility method (SCAM) revealed a series of $\beta2$ strand residues within loop D that are accessible within the binding pocket. Consistent with its role in agonist binding, residue 64 became less accessible to methanethiosulphonate (MTS) modification when receptors were activated by GABA. Residues within the $\alpha1$ subunit $\beta1$ strand are probably also solvent accessible through the ligand-binding pocket because they lie adjacent to the $\beta2$ strand. As a result, Cys-substituted $\beta1$ strand residues may also be amenable to SCAM.

In the present study, we first examined solvent access to the $GABA_A$ $\beta3$ homopentamer using molecular dynamics (MD) simulation. We subsequently used the simulations as a guide to investigate the functional consequences of Cys substitutions at five of the equivalent $\beta1$ strand residues in the $\alpha1$ subunit of $\alpha1\beta2\gamma2$ $GABA_A$ receptors. The introduction of Cys at these positions enabled us to examine their accessibility in the absence and presence of receptor activation.

Methods

Cell culture and transfection

Human embryonic kidney 293 (HEK-293) cells were maintained in Dulbecco's modified Eagle's medium (DMEM) supplemented with 10% fetal bovine serum and

100 μg ml^{-1} penicillin and 100 units ml^{-1} streptomycin at 37°C and 5 % CO_2. Cells were seeded at low density in 35 mm dishes for electrophysiology. Transfections were performed by calcium phosphate precipitation, using 1 μg of total cDNA per dish, as described previously (Baptista-Hon *et al.* 2013). cDNAs encoding wild-type (WT) and mutant mouse $GABA_A$ subunits were in the pRK5 mammalian expression vector. For heteromeric expression of $GABA_A$ $\alpha1\beta2\gamma2$ subunits, a 1:1:1 transfection ratio was used. cDNA encoding enhanced green fluorescent protein (in pEGFP vector, 0.1 μg) was included to identify successfully transfected cells using fluorescence microscopy. Cells were washed with media 16 h after transfection and used after 48–72 h. All tissue culture reagents were obtained from Invitrogen (Paisley, UK).

Mutagenesis of $GABA_A$ $\alpha1$ subunits

Single point mutations were performed by overlap extension PCR (Heckman & Pease, 2007). PCR products were digested using *Sma*I restriction endonuclease and ligated into pRK5 vector. All mutagenesis reactions and ligations were verified using agarose gel electrophoresis and constructs were sequenced prior to functional characterization (Genetics Core Services, University of Dundee, Dundee, UK). All PCR and molecular cloning reagents were obtained from Fermentas (Thermo-Fisher, Loughborough, UK).

Electrophysiology

The whole-cell configuration of the patch clamp technique was used to record GABA-evoked currents from HEK-293 cells expressing WT $\alpha1\beta2\gamma2$ $GABA_A$ receptors or receptors containing Cys-substituted $\alpha1$ subunits. Recording electrodes were fabricated from borosilicate glass capillaries, which, when filled with intracellular solution, had resistances of 1.3 – 2.3 MΩ for whole-cell recordings. The electrode solution contained (in mM): 140 CsCl, 2 $MgCl_2$, 1.1 EGTA, 3 Mg-ATP, 10 Hepes (pH 7.4 with CsOH). The extracellular solution contained (in mM): 140 NaCl, 4.7 KCl, 1.2 $MgCl_2$, 2.5 $CaCl_2$, 10 Hepes, 10 glucose (pH 7.4 with NaOH). Cells were voltage clamped at an electrode potential of –60 mV. Currents were evoked by rapid application of GABA using the three-pipe Perfusion Fast Step system (Warner Instruments, San Francisco, CA, USA), as described previously (Baptista-Hon *et al.* 2013).

All electrophysiological data were recorded using an Axopatch 200B amplifier (Axon Instruments, Burlingame, CA, USA). Data were low pass filtered at 2 kHz, digitized at 20 kHz using a Digidata 1320 A interface and acquired using pCLAMP8 software (all from Molecular Devices, Sunnyvale, CA, USA).

SCAM

The cysteine sulfhydryl-specific modifying effect of a MTS reagent was determined using 2-aminoethyl methanethiosulphonate (MTSEA) or phenylmethanethiosulphonate (PhMTS) (Toronto Research Chemicals, Toronto, Ontario, Canada). Unless otherwise indicated, HEK-293 cells transfected with WT or Cys-substituted subunits were exposed repeatedly to an EC_{50} concentration of GABA to evoke stable baseline currents ($I_{control}$). Freshly diluted MTSEA (up to 10 mM) was then applied episodically to cells prior to their GABA EC_{50} exposure. Altered current amplitudes following MTSEA exposure reveals accessibility to sulfhyrdryl modification ($I_{modified}$). The extent of modification was measured as a percentage change:

$$\%\ \text{change} = \frac{I_{\text{modified}} - I_{\text{control}}}{I_{\text{control}}} \times 100$$

Cells were subsequently exposed to the reducing agent dithiothreitol (DTT) (10 mM) to reverse modification by MTSEA.

Rates of MTSEA modification were measured using empirically determined concentrations of MTSEA that produced cumulative changes in the amplitude of GABA-evoked currents reaching steady-state within the duration of the recording. MTSEA was applied episodically for intervals between 0.1 and 2 s, prior to a challenge with EC_{50} GABA. In all cases, the steady-state current amplitude reached that of $I_{modified}$ when a saturating concentration of MTSEA was used, indicating that the modification reaction had reached completion. To determine whether the rate of MTSEA modification of the substituted cysteine can be altered in the presence of orthosteric agonists or allosteric agonists, a maximal concentration of GABA (EC_{100}), or an activating concentration of propofol (10 μM) was simultaneously applied with MTSEA.

MD simulations

MD simulations were carried out with the simulation software Gromacs, version 4.67 (Pronk *et al.* 2013). The ambersb99_ildn force field (Hornak *et al.* 2006; Lindorff-Larsen *et al.* 2010) for amino acids and the Berger force field for POPC lipids (Berger *et al.* 1997) were applied. Temperature and pressure were kept constant at 298 K and 1 bar, using the v-rescale thermostat (Bussi *et al.* 2007) and the Parrinello-Rahman barostat (Parrinello & Rahman, 1981) with coupling constants of 0.5 and 2 ps, respectively. Electrostatic interactions were computed using the Particle mesh Ewald method with a real space cut-off of 12 Å. Van der Waals interactions were calculated using a cut-off of 12 Å. The LINCS algorithm (Hess *et al.* 1997) was applied to constrain all bonds. Virtual sites

(Feenstra *et al.* 1999) were employed for hydrogen atoms, permitting the use of a simulation timestep of 5 fs. The total sampling time was 1.64 μs.

pK_a values of all titrable groups of the $GABA_A$ $\beta3$ homopentamer (Protein Data Bank code: 4COF) (Miller & Aricescu, 2014) were calculated using the H++ webserver (Anandakrishnan *et al.* 2012). The transmembrane domain of the protein was first aligned to a POPC bilayer, using LAMBADA (Schmidt & Kandt, 2012) and slightly moved manually to match protein–lipid interactions (Contreras *et al.* 2011). The protein was inserted into the membrane, employing the software InflateGRO2 (Schmidt & Kandt, 2012). A NaCl concentration of ~180 mM was added and additional counter ions were introduced to neutralize the simulation system.

Data analysis

The peak amplitudes of agonist-evoked currents were measured using Clampfit, version 10 (Molecular Devices). Individual relationships of current amplitude to GABA concentration were fitted with a logistics equation:

$$f([GABA]) = \frac{100}{1 + 10^{(logEC_{50} - [GABA] \times n^H)}}$$

from which GABA EC_{50} and Hill slope (n^H) values were determined.

The rate of MTSEA modification of Cys-substituted receptors was measured by fitting single or double exponential functions to peak current amplitude data following cumulative MTSEA applications. The double exponential function is defined by:

$$f(t) = Plateau + A_f e^{-t/\tau_f} + A_s e^{-t/\tau_s}$$

where τ_f and τ_s represent the fast and slow time constants, respectively. A_f and A_s represent the proportion of the fast and slow components, respectively, such that A_f and A_s sum to 1 – *Plateau*. Rates of MTSEA modification are provided as weighted τ (τ_w) values, calculated using:

$$\tau_w = A_f \times \tau_f \times A_s \times \tau_s$$

Pseudo first-order rate constants were derived from a modified single or double exponential fit to peak current amplitude data following MTSEA applications. The double exponential function is defined by:

$$f(t) = Plateau + A_f \times e^{(K_f \times t)} + A_s \times e^{(K_s \times t)}$$

where K_f and K_s represent the fast and slow first-order rates, respectively. A_f and A_s represent the proportion of the fast and slow components. Because all amplitude data are normalized to I_{GABA} at $t = 0$, A_f and A_s sum to 1 – *Plateau*. Second-order rate constants were obtained by dividing K by the concentration of MTSEA used (Holden & Czajkowski, 2002).

The solvent accessible surface area (SASA) was calculated as described previously (Eisenhaber *et al.* 1995) using data from the MD simulations. The solvent accessible area was graphically represented using trj_cavity (Paramo *et al.* 2014). All figures containing molecular information were produced using VMD (Humphrey *et al.* 1996).

Statistical analysis

Data are presented as the mean ± SEM or SD as indicated. Differences in means of three or more groups were compared using one-way ANOVA, with a *post hoc* Tukey or Dunnet's test, as appropriate. Pairwise comparisons were performed using Student's *t* test. $P < 0.05$ was considered statistically significant. Statistical analyses were performed using Prism, version 5 (GraphPad Software, San Diego, CA, U.S.A.).

Results

Residues in the $\beta1$ strand of the $\beta3$ homopentamer are solvent accessible

Changes in the accessibility of residues during $GABA_A$ receptor activation have been determined using SCAM (Boileau *et al.* 1999). Two criteria are required for successful SCAM. First, the substituted Cys must be solvent accessible and, second, it must participate in a receptor function that is affected by modification. Both of these criteria apply to the $GABA_A$ receptor $\alpha1$ subunit $\beta2$ strand loop D residue at position 64. This residue is solvent accessible and its modification by MTS reagents led to a reduction in GABA-evoked current amplitudes in receptors harbouring the $\alpha1$(F64C) substitution (Boileau *et al.* 1999). Phe64 participates in GABA binding and efficacy (Boileau *et al.* 1999; Szczot *et al.* 2014). Although residues in the $\beta1$ strand do not participate in agonist binding to the $GABA_A$ $\beta3$ homopentamer structure, we examined whether they are accessible through the binding pocket (Miller and Aricescu, 2014). We performed MD simulations of the whole protein but focused our analysis on residues located within the $\beta1$ strand of the $\beta3$ homopentamer (Fig. 1*A*).

Our simulations reveal that a number of residues in the $\beta1$ strand of the $GABA_A$ β_3 homopentamer are solvent accessible. A representative snapshot of the access pathways of water to the agonist binding site observed in the simulations is shown in Fig. 1*B*. Consistent with previous reports, the critical $\beta2$ strand loop D residue, equivalent to 64 in the $\alpha1$ subunit, which is

Tyr62 in the $\beta3$ homopentamer, is also accessible. We quantified the SASA for these residues (Fig. 1*C*). The SASA values for residues from 41 to 45 are characteristic of a β-strand structure with an alternating pattern of accessibility. While residues Asn41, Asp43 and Ala45 display significant solvent accessibility, Ile42 and Ile44 are inaccessible. The number of water molecules observed to be in contact with the residues throughout our simulations agrees well with their SASA (data not shown). Other residues (e.g. Cys37, Ser46, Asp48, Met49 and Ser51) also have significant SASA values and may therefore be accessible. However, inspection of the model reveals that the highly accessible Cys37 and Met49 are located outside the binding pocket at the surface of the receptor and within the outer vestibule, respectively. Furthermore, in the $\beta3$ homopentamer model, the $\beta1$ strand has a sharp kink after residue 45, dipping towards the vestibule.

$\beta1$ strand residues influence the apparent potency of GABA

Our MD simulations (Fig. 1) suggest that several residues within the $\beta1$ strand of $GABA_A$ receptors are part of a solvent accessible pocket contiguous with the ligand-binding domain. We investigated the functional consequences of individual Cys substitutions from Asp43 to Thr47 in the $\alpha1$ subunit. These residues are homologous to those between Asn41 and Ala45 in the $GABA_A$ $\beta3$ homopentamer according to our sequence alignment (Fig. 1*A*). For comparison, we also included Cys-substituted Phe64 in loop D of the $\beta2$ strand in our analysis. WT or Cys-substituted $\alpha1$ subunits were transiently expressed in HEK-293 cells with $\beta2$ and $\gamma2$ subunits. Representative examples of GABA-evoked currents mediated by Cys-substituted $GABA_A$ receptors are shown in Fig. 2*A*.

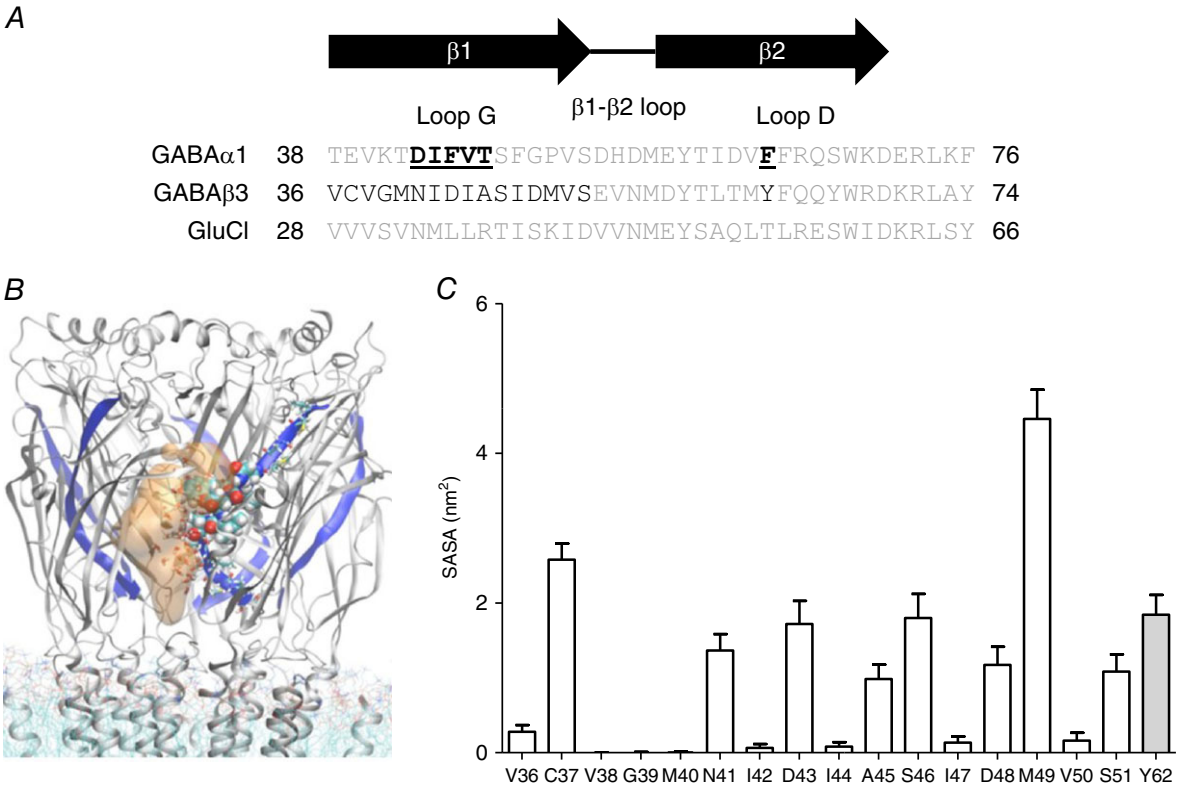

Figure 1. Amino acids implicated in agonist binding to $GABA_A$ and GluCl receptors in $\beta1$ and $\beta2$ strands, respectively
A, amino acid sequence alignment of the mouse $GABA_A$ $\alpha1$ and $\beta3$ subunits, and the *C. elegans* GluCl α subunit. The region shown in the sequence alignment contains the residues relevant to the present study. Residues in the $GABA_A$ $\beta3$ subunit evaluated using MD simulations are shown in black. The residues in the $\beta1$ strand of the $\alpha1$ subunit mutated to Cys are bold and underlined. *B*, graphical representation of the solvent accessible area of the $GABA_A$ β_3 homopentamer from a representative snapshot. The $\beta1$ strand is shown in blue in all five subunits, residues of particular interest in one subunit are displayed as van der Waals spheres, and water molecules within a distance of 4.5 Å of these residues are shown as sticks. The solvent accessible crevice near the $\beta1$ strand is displayed in orange (transparent). *C*, SASA of $\beta1$ strand residues and Tyr62 (equivalent to $\alpha1$ subunit Phe64) in the $GABA_A$ β_3 homopentamer. The SASA of the homologous residues chosen for functional analysis are (mean ± SD): 1.34 ± 0.2 nm^2 for Asn41, 0.05 ± 0.04 nm^2 for Ile42, 1.85 ± 0.26 nm^2 for Asp43, 0.07 ± 0.06 nm^2 for Ile44 and 1.07 ± 0.18 nm^2 for Ala45 in the $\beta1$ strand. Tyr62 in loop D of the $\beta2$ strand had a SASA of 1.93 ± 0.2 nm^2.

GABA concentration–response relationships are plotted in Fig. 2*B*. Logistic functions fitted to the data reveal rightward shifts in the GABA concentration–response relationship for some Cys-substituted receptors. The average best-fit parameters derived from logistic functions fitted to data recorded from several different cells are summarized in Table 1. Consistent with previous studies, $\alpha1$(F64C)$\beta2\gamma2$ receptors displayed a large increase in EC_{50} ($P < 0.0001$; *t* test *vs.* WT $\alpha1\beta2\gamma2$ receptors), confirming an important role for this $\beta2$ strand residue in $GABA_A$ receptor function. For $\beta1$ strand Cys-substituted $\alpha1\beta2\gamma2$ receptors, one-way ANOVA with a Dunnet's comparison revealed a significant difference in GABA EC_{50} between $\alpha1$(D43C)$\beta2\gamma2$ and WT $\alpha1\beta2\gamma2$ receptors ($P < 0.0001$) (Table 1). $\alpha1$(I44C)$\beta2\gamma2$ and $\alpha1$(T47C)$\beta2\gamma2$ receptors showed tendencies towards increased EC_{50} values, although these were not significantly different from WT. $\alpha1$(V46C)$\beta2\gamma2$ receptors had EC_{50} values indistinguishable from WT $\alpha1\beta2\gamma2$ receptors. The Hill slope values for these Cys-substituted $GABA_A$ receptors were similar to that of WT $\alpha1\beta2\gamma2$ receptors (Table 1). Similar to $\alpha1$(F64C)$\beta2\gamma2$, both $\alpha1$(D43C)$\beta2\gamma2$ and $\alpha1$(T47C)$\beta2\gamma2$ receptors had reduced GABA-evoked peak current densities compared to WT, which were statistically significant ($P < 0.0001$ and $P < 0.05$, respectively; one-way ANOVA with *post hoc* Dunnet's comparison with $\alpha1\beta2\gamma2$ receptors) (Table 1). The Cys substitution in $\alpha1$(F45C)$\beta2\gamma2$ receptors produced more complicated changes in function, which are described below.

The $\alpha1$ F45C substitution causes a biphasic GABA concentration–response relationship and spontaneous gating

The GABA concentration–response relationship for $\alpha1$(F45C)$\beta2\gamma2$ receptors is shown in Fig. 3*A*, along with representative examples for GABA-evoked currents. A single component logistic function provided an inadequate representation of the concentration–response relationship for GABA-evoked currents mediated by $\alpha1$(F45C)$\beta2\gamma2$ receptors. By contrast, a two-component logistic function provided a good fit across the entire GABA concentration range (Fig. 3*A*, solid black line). An *F* test applied to statistically discriminate between the two approaches revealed that the two-component logistic function provided a significantly improved fit to the data ($P = 0.025$). The solid grey lines in Fig. 3*A* illustrate the two components of the GABA concentration–response relationship. The logistic fit for WT $\alpha1\beta2\gamma2$ receptors is also reproduced here (dashed grey line) for comparison. Table 1 contains the values derived from the two-component logistic function consistent

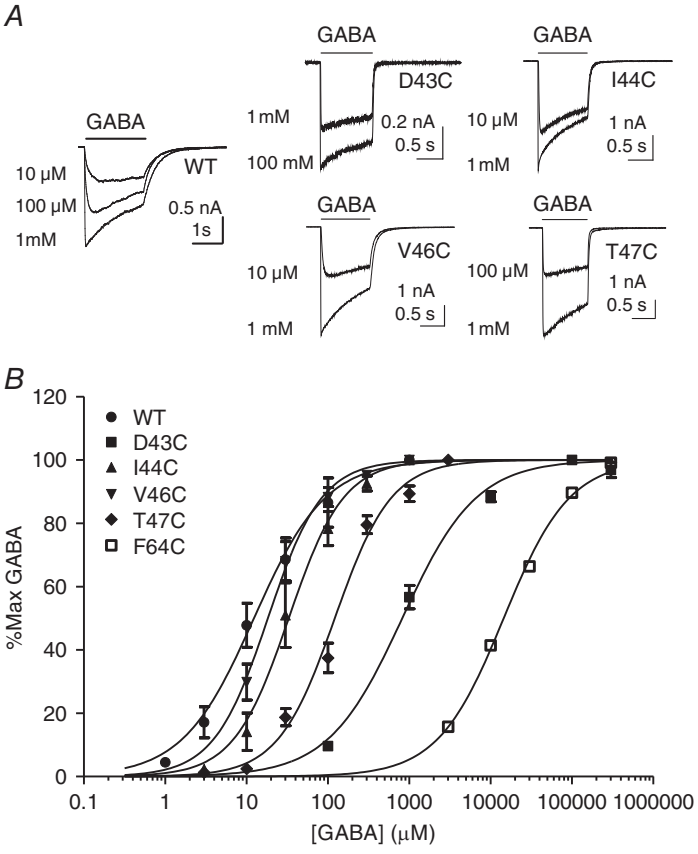

Figure 2. $\beta1$ strand residues influence the apparent potency of GABA
A, representative examples of whole-cell currents evoked by different concentrations of GABA (indicated) mediated by WT or Cys-substituted $\alpha1\beta2\gamma2$ receptors. The bar indicates GABA application. *B*, concentration–response relationships for WT or Cys-substituted $\alpha1\beta2\gamma2$ $GABA_A$ receptors. Current amplitudes are expressed as a percentage of the maximum current amplitude recorded from each cell. Each point represents the mean ± SEM of at least four recordings. The sigmoidal curve represents the logistic function fitted to the data points. Mean parameters and statistical comparisons from the logistic function are summarized in Table 1.

Table 1. Summary of logistic function fit parameters and current density values

	GABA EC_{50} (μM)	Hill slope	Current density (pA pF^{-1})
$\alpha1\beta2\gamma2$	17.8 ± 5.1 (6)	1.12 ± 0.17 (6)	1400 ± 250 (20)
$\alpha1$(D43C)$\beta2\gamma2$	857 ± 161 (5)*	1.01 ± 0.059 (5)	210 ± 69 (8)*
$\alpha1$(I44C)$\beta2\gamma2$	38.4 ± 11.7 (5)	1.68 ± 0.15 (5)	1200 ± 330 (7)
$\alpha1$(F45C)$\beta2\gamma2$	HP 0.52 (16) LP 150 (16)	HP 1.91 (16) LP 0.51 (16)	880 ± 130 (27)
$\alpha1$(V46C)$\beta2\gamma2$	19.0 ± 4.1 (4)	1.48 ± 0.13 (4)	890 ± 230 (7)
$\alpha1$(T47C)$\beta2\gamma2$	135 ± 13.7 (9)	1.42 ± 0.20 (9)	610 ± 110 (12)*
$\alpha1$(F64C)$\beta2\gamma2$	19000 ± 1600 (3)†	1.00 ± 0.29 (3)	77.9 ± 33.3 (13)†

Data are provided as the mean ± SEM of (*n*) number of experiments, except EC_{50} and Hill slope values of $\alpha1$(F45C)$\beta2\gamma2$ receptors, where the average fit parameters of the high apparent potency (HP) and low apparent potency (LP) components are reported. *Significant difference ($P < 0.05$) from one-way ANOVA with Dunnet's *post hoc* comparison with $\alpha1\beta2\gamma2$ values. $\alpha1$(F45C)$\beta2\gamma2$ receptors were not statistically compared for EC_{50} and Hill slope values because of the presence of two components in the GABA concentration–response relationship. †Significant difference ($P < 0.05$) between $\alpha1$(F64C)$\beta2\gamma2$ receptors and $\alpha1\beta2\gamma2$ receptors from *t* test.

with high and low apparent potency components for GABA-evoked activation of $\alpha1$(F45C)$\beta2\gamma2$ receptors.

$GABA_A$ receptors with high levels of spontaneous gating generally have a higher sensitivity to GABA (Mortensen *et al.* 2003; Hadley & Amin, 2007). The high apparent potency component of GABA activation of $\alpha1$(F45C)$\beta2\gamma2$ receptors may therefore be associated with spontaneous activity. We investigated the possibility of spontaneous gating by recording the inhibition of basal currents by picrotoxin (PTX) in WT $\alpha1\beta2\gamma2$ and $\alpha1$(F45C)$\beta2\gamma2$ receptors. Figure 3*B* shows representative examples of maximally effective GABA-evoked currents (grey trace) and inhibition of basal currents by PTX (black trace). WT $\alpha1\beta2\gamma2$ receptors display very little PTX inhibited basal current (Fig. 3*B* inset). By comparison, the magnitude of PTX inhibited basal current in $\alpha1$(F45C)$\beta2\gamma2$ receptors was large (Fig. 3*B*, inset). We quantified spontaneous current as the magnitude of the PTX component (I_{PTX}) expressed as a percentage of the total amount of current ($I_{GABA} + I_{PTX}$). The maximum GABA-evoked current densities in WT $\alpha1\beta2\gamma2$ and $\alpha1$(F45C)$\beta2\gamma2$ receptors did not differ significantly (Table 1). Therefore, the maximum efficacy of GABA is probably not altered by the F45C substitution. The mean I_{PTX}/I_{total} values are shown in Fig. 3*C*. $\alpha1$(F45C)$\beta2\gamma2$ receptors had an increased proportion of spontaneous current from 0.05 ± 0.02% ($n = 5$) in WT $\alpha1\beta2\gamma2$ receptors to 0.52 ± 0.11% ($n = 10$). The difference was statistically significant ($P = 0.014$; *t* test). These data suggest that F45C substitution increased spontaneous gating and therefore Phe45 in the $\beta1$ strand plays critical and complex roles in $GABA_A$ receptor function.

Several residues in the $\beta1$ strand of the $GABA_A$ $\alpha1$ subunit are accessible to MTSEA modification

$\beta1$ strand residues in the GluCl α subunit (Hibbs & Gouaux, 2011) and $GABA_A$ $\beta3$ homopentamer (Miller & Aricescu, 2014) models have side chains facing into the orthosteric binding pocket. Our MD simulation data demonstrate that residues in the $GABA_A$ $\beta3$ homopentamer, equivalent to amino acids 43–47 in the $\alpha1$ subunit, are solvent accessible (Fig. 1*C*). Furthermore, receptors containing $\alpha1$ subunit D43C, F45C and T47C substituents all exhibit functions distinguishable from WT receptors (Figs 2 and 3 and Table 1). Therefore, $\alpha1$ subunit $\beta1$ strand residues may be accessible to MTS reagents and their modification may alter function.

We used SCAM to investigate whether the substituted cysteine residues in the $\beta1$ strand of the $GABA_A$ receptor are accessible to the sulfhydryl reagent, MTSEA. The use of a similar approach previously in *Xenopus* oocytes demonstrated the accessibility of substituted cysteines in $\alpha1$(F64C) containing $GABA_A$ receptors (Boileau *et al.* 1999; Holden & Czajkowski, 2002). We adapted the technique for use in whole-cell patch clamp recordings from HEK-293 cells using rapid application of GABA and MTSEA (see Methods), and used $\alpha1$(F64C)$\beta2\gamma2$ receptors for comparison.

We first tested whether MTSEA (10 mM) modulates $GABA_A$ receptors containing WT $\alpha1$ subunits (Fig. 4*A*). Control currents were evoked by an EC_{50} concentration of GABA (10 μM) in HEK-293 cells expressing $\alpha1\beta2\gamma2$ $GABA_A$ receptors. Modification by MTSEA (10 mM) was tested by pre-application for 2 s prior to GABA. Five applications were tested, such that cells were exposed to MTSEA cumulatively for 10 s. The amplitudes of GABA-evoked currents appeared modestly enhanced following MTSEA treatment in some cells, although the mean did not significantly differ from that of controls ($n = 6$). We next confirmed that MTSEA (2 mM) modifies the function of $\alpha1$(F64C)$\beta2\gamma2$ receptors. MTSEA substantially reduced the current amplitude evoked by an EC_{50} concentration of GABA (10 mM) (Fig. 4*A*). The application of the reducing agent DTT (10 mM) reversed the modification by MTSEA. This result is consistent with

the results of a previous study of the effects of SCAM on $GABA_A$ receptors containing the α1(F64C) subunit (Boileau *et al.* 1999).

Using the same approach, we applied MTSEA (10 mM) to $GABA_A$ receptors containing Cys-substituted β1 strand residues. Exemplar currents evoked by an EC_{50} concentration of GABA before and after MTSEA application are shown in Fig. 4*B*. MTSEA application caused a reduction in GABA-evoked current amplitude in α1(D43C)β2γ2 and α1(T47C)β2γ2 receptors. MTSEA did not affect the amplitude of α1(I44C)β2γ2, α1(F45C)β2γ2 or α1(V46C)β2γ2 receptors. The equivalent residues to Cys44 and Cys46 in the $GABA_A$ β3 homopentamer showed low SASA values and the failure of MTSEA to affect function is consistent with their lack of solvent accessibility (Fig. 1*C*).

It is interesting that α1(F45C)β2γ2 receptors were unaffected by MTSEA despite a high SASA (Fig. 1*C*) and the importance of the identity of this residue in receptor function (Fig. 3). It is possible that modification by MTSEA, which would add a positive charge to the Cys residue, was functionally silent in these receptors. We therefore used a different sulfhydryl modifying reagent, PhMTS, which adds an aromatic group to an accessible Cys, a modification that would mimic the native Phe. However, PhMTS (200 μM) applied for more than 2 min also had no effect on the function of α1(F45C)β2γ2 receptors (data not shown). In addition, we repeated the

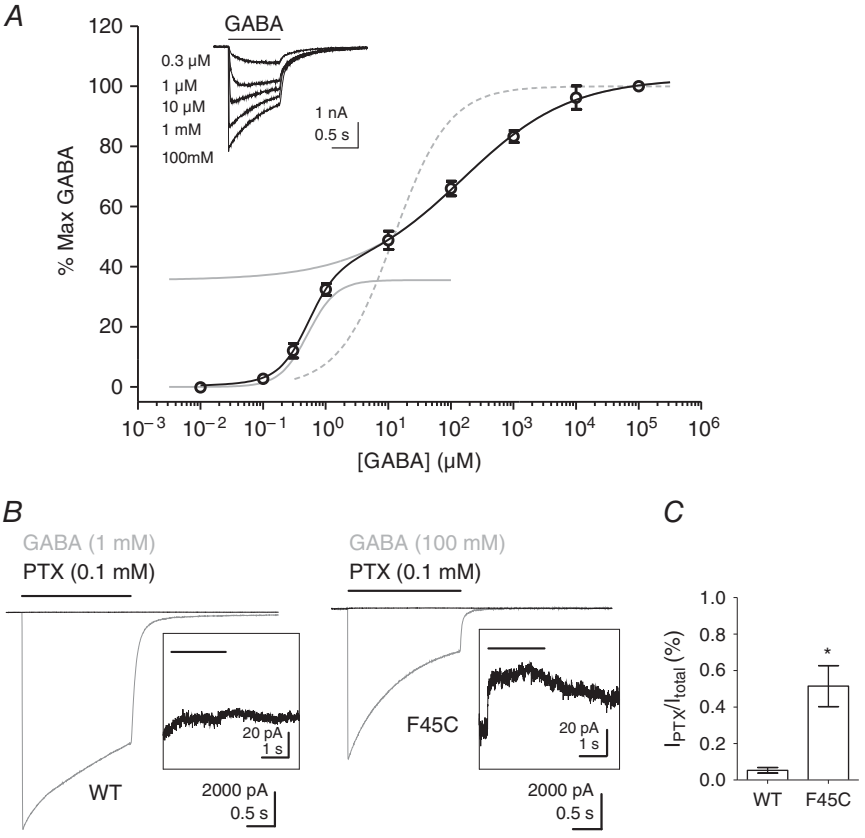

Figure 3. α1(F45C)β2γ2 $GABA_A$ receptors display a biphasic GABA concentration–response relationship and are more spontaneously active
A, concentration–response relationship for α1(F45C)β2γ2 $GABA_A$ receptors. Current amplitudes are expressed as a percentage of maximum. Each point represents the mean ± SEM of at least four recordings. The solid black line shows the two component logistic function fit to the data points. The two solid grey lines show the separate components of the logistic function fit. The fit parameters are summarized in Table 1. The logistic function fit for WT α1β2γ2 receptors is also reproduced for comparison (grey dotted line). Inset shows a representative example of whole-cell currents evoked by different concentrations of GABA (indicated) mediated by α1(F45C)β2γ2 $GABA_A$ receptors. The bar indicates GABA application. *B*, representative examples of whole-cell currents evoked by a maximally efficacious concentration of GABA (grey traces) or inhibition of standing current by PTX (black trace) at α1β2γ2 or α1(F45C)β2γ2 receptors. The black bar indicates GABA or PTX application. The inset shows, on an expanded scale, PTX inhibition of standing current. *C*, graph showing mean ± SEM PTX inhibited standing current (I_{PTX}) expressed as a percentage of the total current (I_{total}) for α1β2γ2 ($n = 5$) and α1(F45C)β2γ2 ($n = 10$) $GABA_A$ receptors. The difference in mean PTX component was significantly higher at α1(F45C)β2γ2 receptors (*$P = 0.014$; *t* test).

MTSEA experiment on $\alpha1(F45C)\beta2\gamma2$ receptors using 1 mM GABA as the test concentration. The effect of 1 mM GABA was maximal at WT $\alpha1\beta2\gamma2$ receptors (Fig. 2*C*), whereas this concentration was only 80% effective at $\alpha1(F45C)\beta2\gamma2$ receptors (Fig. 3*A*). However, MTSEA had no effect on the amplitude of GABA (1 mM)-evoked currents (data not shown). In addition to an altered GABA concentration–response relationship, $\alpha1(F45C)\beta2\gamma2$ receptors displayed higher spontaneous activity compared to WT $\alpha1\beta2\gamma2$ receptors. We therefore examined whether MTSEA could influence the extent of spontaneous activity mediated by $\alpha1(F45C)\beta2\gamma2$ receptors. Cells were treated with MTSEA (2 mM) for 2 min and spontaneous activity was measured as the percentage

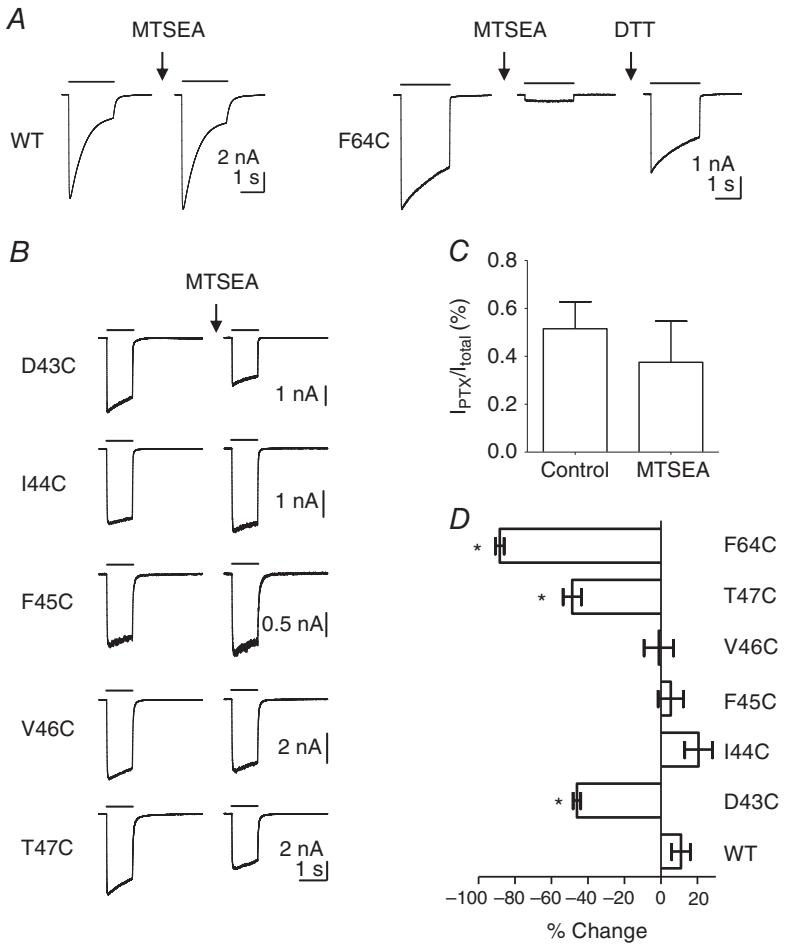

Figure 4. Accessibility of Cys-substituted $\beta1$ strand residues to sulfhydryl modification
A, representative examples of the effect of MTSEA on WT $\alpha1\beta2\gamma2$ and $\alpha1(F64C)\beta2\gamma2$ receptors. MTSEA (10 mM) was applied to a cell expressing WT $\alpha1\beta2\gamma2$ receptors prior to recording a current evoked by the EC_{50} concentration (10 μM, black bar) of GABA. Also shown is the effect of MTSEA (2 mM) on $\alpha1(F64C)\beta2\gamma2$ receptors. MTSEA substantially reduced the amplitude of the EC_{50} (10 mM) GABA-evoked (black bar) current through $\alpha1(F64C)\beta2\gamma2$ receptors. Modification was reversed following application of DTT (10 mM). *B*, representative examples of MTSEA (2 mM) on $\beta1$ strand Cys-substituted $\alpha1\beta2\gamma2$ receptors. MTSEA (arrow) reduced the current amplitude of $\alpha1(D43C)\beta2\gamma2$ and $\alpha1(T47C)\beta2\gamma2$ receptors. *C*, effect of MTSEA (2 mM) on spontaneous activity of $\alpha1(F45C)\beta2\gamma2$ receptors. Spontaneous activity was quantified as the I_{PTX}/I_{total}. The level of spontaneous activity under control conditions was 0.51 ± 0.11% ($n = 10$). In the presence of MTSEA (2 mM), the level of spontaneous activity was 0.38 ± 0.17% ($n = 5$). The difference was not statistically significant. ($P > 0.05$; *t* test). *D*, graph showing mean ± SEM percentage change in current amplitude following MTSEA treatment in WT and mutant $\alpha1\beta2\gamma2$ receptors. The change in GABA-evoked current amplitude was 11 ± 5.1% ($n = 6$) for WT $\alpha1\beta2\gamma2$, –46 ± 2.1% ($n = 8$) for $\alpha1(D43C)\beta2\gamma2$, 21 ± 7.5% ($n = 3$) for $\alpha1(I44C)\beta2\gamma2$, 5.4 ± 6.9% ($n = 4$) for $\alpha1(F45C)\beta2\gamma2$, –1.1 ± 8.1% ($n = 3$) for $\alpha1(V46C)\beta2\gamma2$, –49 ± 5.0% ($n = 15$) for $\alpha1(T47C)\beta2\gamma2$ and –88 ± 2.4% ($n = 4$) for $\alpha1(F64C)\beta2\gamma2$ receptors. There was a statistically significant difference in the percentage change between $\alpha1(D43C)\beta2\gamma2$, $\alpha1(T47C)\beta2\gamma2$ and $\alpha1(F64C)\beta2\gamma2$ receptors compared to WT $\alpha1\beta2\gamma2$, receptors (*$P < 0.0001$; one-way ANOVA; *post hoc* Dunnet's comparison *vs*. WT).

of I_{PTX} to I_{total}. Figure 4*C* shows I_{PTX}/I_{total} under control conditions and in the presence of MTSEA (2 mM). There was no significant difference in the level of spontaneous activity in the presence of MTSEA. Taken together, these data suggest that, although Cys43 and Cys47 are accessible to MTSEA, Cys45 is inaccessible.

We quantified the extent of MTSEA modification determining the percentage changes in EC_{50} GABA-evoked current amplitude for each Cys-substituted receptor before and after MTSEA application. These values are plotted in Fig. 4*D*. Application of MTSEA caused a significant reduction in the amplitudes of GABA-evoked currents mediated by $\alpha1$(D43C)$\beta2\gamma2$, $\alpha1$(T47C)$\beta2\gamma2$ and $\alpha1$(F64C)$\beta2\gamma2$ receptors relative to those mediated by WT receptors ($P < 0.0001$; one-way ANOVA; *post hoc* Dunnet's comparison *vs.* $\alpha1\beta2\gamma2$).

Receptor activation influences MTSEA modification of D43C and T47C containing receptors

Receptor activation by an agonist might influence the accessibility of a substituted Cys. This could occur as a result of the bound agonist directly protecting the residue from modification. Alternatively, activation may cause a conformational rearrangement of the receptor in which the Cys becomes less accessible. The $\alpha1$(F64C) was modified more slowly by an MTS reagent applied with GABA to *Xenopus* oocytes expressing $\alpha1$(F64C)$\beta2\gamma2$ receptors (Boileau *et al.* 1999). We investigated whether GABA also affects the modification of $\alpha1$(D43C)$\beta2\gamma2$ and $\alpha1$(T47C)$\beta2\gamma2$ receptors by applying MTSEA in its presence and absence. Once again, we modified the approach for use in voltage clamped HEK-293 cells (see Methods).

First, using this approach, we compared the rate of MTSEA modification of $\alpha1$(D43C)$\beta2\gamma2$, $\alpha1$(T47C)$\beta2\gamma2$ and $\alpha1$(F64C)$\beta2\gamma2$ receptors. Figure 5*A* shows representative examples of the effect of rapid and short applications of MTSEA on GABA-evoked currents mediated by $\alpha1$(D43C)$\beta2\gamma2$, $\alpha1$(T47C)$\beta2\gamma2$ and $\alpha1$(F64C)$\beta2\gamma2$ receptors. The concentration of MTSEA used for each mutant was chosen empirically on the basis of a measurable reduction in the amplitude of the EC_{50} GABA-evoked current during the time course of the experiment. For $\alpha1$(D43C)$\beta2\gamma2$ and $\alpha1$(F64C)$\beta2\gamma2$ receptors, MTSEA (100 μM and 10 μM, respectively) was applied episodically for 100 ms, prior to application of a test concentration of GABA (EC_{50}). For both receptors, the modification was complete within 500 ms. The rate of MTSEA (100 μM) modification of $\alpha1$(T47C)$\beta2\gamma2$ receptors was slower and therefore MTSEA was applied episodically for 500 ms prior to the application of GABA (EC_{50}). We analysed the change in EC_{50} GABA-evoked current amplitude and expressed these as a percentage of the control current. Figure 5*B* shows the rate of MTSEA evoked reduction of GABA-evoked currents mediated by $\alpha1$(D43C)$\beta2\gamma2$, $\alpha1$(T47C)$\beta2\gamma2$ and $\alpha1$(F64C)$\beta2\gamma2$ receptors. In all cases, the time course of MTSEA modification was well fitted with a single exponential. The mean ± SEM time constants of modification are plotted in Figure 5*C*. One-way ANOVA with a *post hoc* Tukey's comparison of the time constants revealed that both $\alpha1$(D43C)$\beta2\gamma2$ and $\alpha1$(F64C)$\beta2\gamma2$ receptors exhibited significantly smaller modification time constants compared to that of $\alpha1$(T47C)$\beta2\gamma2$ receptors ($P < 0.0001$). We also determined the second-order rate constants for MTSEA modification (see Methods). Second-order rate constants are summarized in Table 2. The second-order rate constants for $\alpha1$(F64C)$\beta2\gamma2$ receptors were significantly faster than those of $\alpha1$(D43C)$\beta2\gamma2$ and $\alpha1$(T47C)$\beta2\gamma2$ receptors ($P < 0.0001$; one-way ANOVA; *post hoc* Tukey's comparison) (Table 2). Our second-order rate constant for MTSEA modification, derived from HEK cells expressing $\alpha1$(F64C)$\beta2\gamma2$ receptors, is similar to that reported by Holden and Czajkowski (2002) in oocytes. The plateau of modification for $\alpha1$(D43C)$\beta2\gamma2$, $\alpha1$(T47C)$\beta2\gamma2$ and $\alpha1$(F64C)$\beta2\gamma2$ receptors, which indicates the maximal extent of functional change for the concentration of MTSEA tested, did not differ from those shown in Figure 4*D*, which used a high concentration of MTSEA (2 mM). This demonstrates that modification was complete. Our data suggest that Cys64 and Cys43 are more accessible to modification than Cys47.

We next repeated the experiment in the presence of either a maximal concentration of GABA or an activating concentration of propofol (10 μM), applied simultaneously with MTSEA. In all cases [$\alpha1$(F64C)$\beta2\gamma2$, $\alpha1$(D43C)$\beta2\gamma2$ and $\alpha1$(T47C)$\beta2\gamma2$ receptors], the co-application of either GABA or propofol with MTSEA induced inward currents. Figure 6*A* shows the rate of MTSEA (10 μM) modification of $\alpha1$(F64C)$\beta2\gamma2$ receptors in the presence of either GABA (300 mM) or propofol (10 μM). The rate of modification was again measured by episodic (100 ms) application of MTSEA (10 μM) with GABA (300 mM) or propofol (10 μM) for the first 500 ms. Propofol did not affect the rate of MTSEA modification (Fig. 6*A*, inset). In the presence of GABA (300 mM), however, the extent of modification following 500 ms of MTSEA exposure was less than in its absence (Fig. 6*A*, inset). We therefore increased the duration of each episodic application to 2 s. The rate of modification in the presence of GABA was best fitted with a double exponential (Fig. 6*A*). The τ_w was calculated for modification when MTSEA was applied simultaneously with GABA and compared with the τ for modification in the absence of GABA. The mean ± SEM time constants are plotted in Fig. 6*B*. The second-order rate constants derived from the exponential fits are summarized in Table 2. GABA (300 mM), but not propofol (10 μM), significantly slowed the rate of MTSEA (10 μM) modification of

$\alpha1$(F64C)$\beta2\gamma2$ receptors ($P = 0.0004$; one-way ANOVA; *post hoc* Tukey's comparison). Our data are consistent with previous observations indicating that GABA, but not the allosteric agonist pentobarbital, influences the modification of $\alpha1$(F64C) containing $GABA_A$ receptors (Boileau *et al.* 1999).

Using the same approach, we determined the effect of GABA and propofol on MTSEA (100 μM) modification of $\alpha1$(D43C)$\beta2\gamma2$ and $\alpha1$(T47C)$\beta2\gamma2$ receptors. The concentrations of GABA used were 300 mM and 30 mM, respectively, and propofol at a concentration of 10 μM was used for both receptors. The time course for MTSEA modification in the control, in the presence of GABA and in the presence of propofol for $\alpha1$(D43C)$\beta2\gamma2$ receptors is shown in Fig. 6*D*. MTSEA in the presence or absence of agonists was applied cumulatively for 100 ms. The rates of modification in all three conditions were well fitted with single exponential functions (Fig. 6*D*). The mean ± SEM time constants and the extent of functional change are plotted in Fig. 6*E* and 6*F*, respectively. Second-order rate

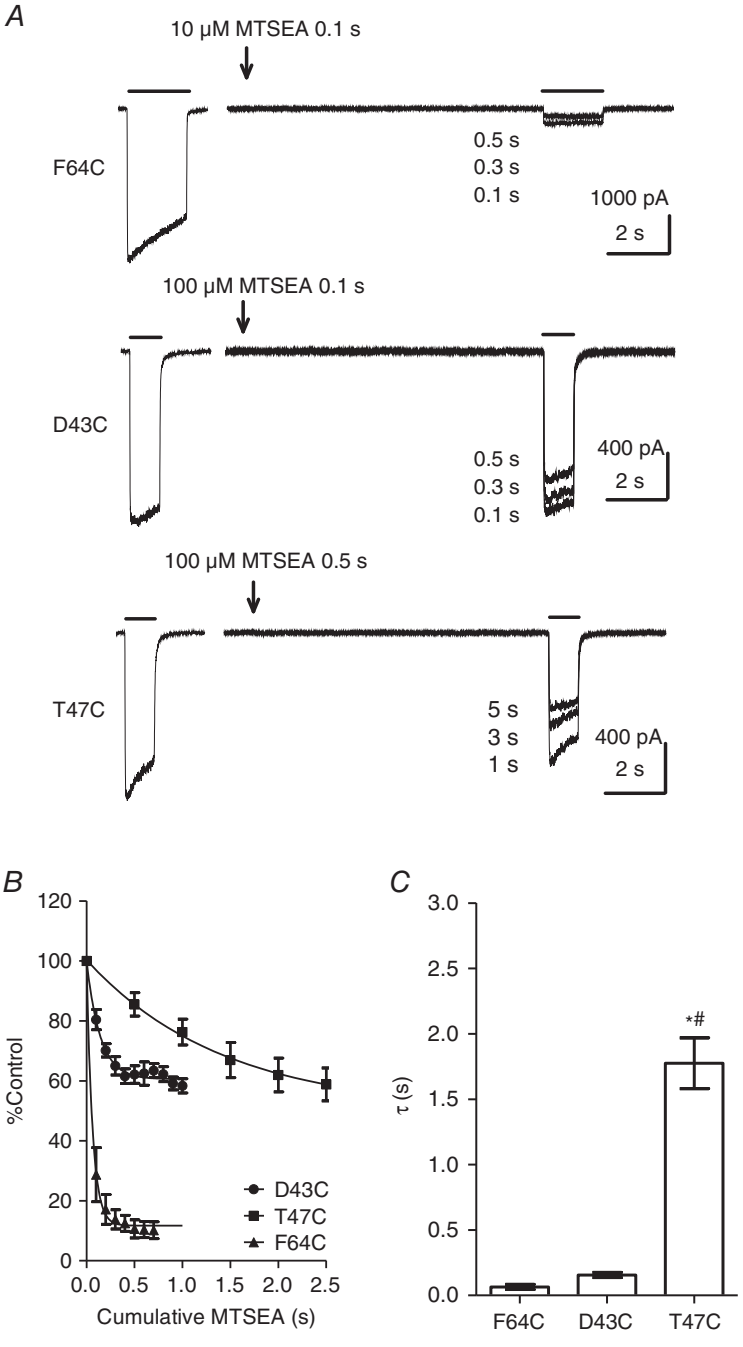

Figure 5. Rate of MTSEA modification of Cys64, Cys43 and Cys47
A, representative examples of EC_{50} GABA-evoked currents before and after cumulative MTSEA application at $\alpha1$(F64C)$\beta2\gamma2$, $\alpha1$(D43C)$\beta2\gamma2$ and $\alpha1$(T47C)$\beta2\gamma2$ receptors. The first current in each trace indicates the steady-state EC_{50} GABA-evoked current amplitude under control conditions. MTSEA was applied for the indicated time (arrow) and a second EC_{50} GABA-evoked current was recorded. Cumulative application of MTSEA led to a progressive reduction in EC_{50} GABA-evoked current amplitudes. *B*, rate of MTSEA modification of $\alpha1$(F64C)$\beta2\gamma2$ ($n = 4$), $\alpha1$(D43C)$\beta2\gamma2$ ($n = 6$) and $\alpha1$(T47C)$\beta2\gamma2$ ($n = 8$) receptors. The line shows the exponential function fitted to the data points. *C*, graph showing mean ± SEM τ of MTSEA modification of $\alpha1$(F64C)$\beta2\gamma2$ (0.065 ± 0.020 s; $n = 4$), $\alpha1$(D43C)$\beta2\gamma2$ (0.16 ± 0.020 s; $n = 6$) and $\alpha1$(T47C)$\beta2\gamma2$ (1.8 ± 0.19 s; $n = 8$) receptors. The τ of MTSEA modification was significantly larger for $\alpha1$(T47C)$\beta2\gamma2$ receptors compared to $\alpha1$(D43C)$\beta2\gamma2$ and $\alpha1$(F64C)$\beta2\gamma2$ receptors ($^{*\#}P < 0.0001$; one-way ANOVA; *post hoc* Tukey's comparison).

Table 2. Summary of second-order rate constants for MTSEA modification

	MTSEA *k2* (M^{-1} s^{-1})	MTSEA + GABA *k2* (M^{-1} s^{-1})	MTSEA + propofol *k2* (M^{-1} s^{-1})
$\alpha1$(D43C)$\beta2\gamma2$	70,030 ± 9,629 (6)	34,530 ± 10,420 (6)*	38,860 ± 8,437 (7)
$\alpha1$(T47C)$\beta2\gamma2$	6,216 ± 784.8 (8)	3,892 ± 873.6 (5)	6,049 ± 1,271 (6)
$\alpha1$(F64C)$\beta2\gamma2$	1,944,000 ± 460,500 (4)†	24,660 ± 9,129 (4)*	1,832,000 ± 205,400 (5)

Data are provided as the mean ± SEM of (*n*) number of experiments. The second-order rate constants are calculated by dividing the rate of decay, obtained from the exponential fits to data that generated the rate of MTSEA modification data, by the concentration of MTSEA used. The concentration of MTSEA used was 100 μM for $\alpha1$(D43C)$\beta2\gamma2$ and $\alpha1$(T47C)$\beta2\gamma2$ receptors, and 10 μM for $\alpha1$(F64C)$\beta2\gamma2$ receptors. *Significant difference ($P < 0.05$) from one-way ANOVA with *post hoc* Tukey's comparison between the presence or absence of saturating concentrations of GABA or activating concentrations of propofol. †Significant difference ($P < 0.05$) from one-way ANOVA with *post hoc* Tukey's comparison between MTSEA *k2* of different mutants.

constants are summarized in Table 2. In the presence of GABA (300 mM), there was a significant increase in the τ of MTSEA modification ($P < 0.05$; one-way ANOVA; *post hoc* Tukey's comparison *vs.* control). There was a tendency for the τ of modification to increase in the presence of propofol, although this was not statistically significant. However, there was also no significant difference in the τ of modification in the presence of GABA and in the presence of propofol. Furthermore, comparison of the extent of functional change revealed a statistically significant reduction between that in the presence of GABA and control ($P < 0.05$; one-way ANOVA; *post hoc* Tukey's comparison *vs.* control), as well as that in the presence of propofol and control ($P < 0.05$; one-way ANOVA; *post hoc* Tukey's comparison *vs.* control) (Fig. 6*F*). These data therefore suggest that both GABA and propofol influence MTSEA modification of Cys43. This is in contrast to Cys64 in loop D where the allosteric agonist propofol did not influence MTSEA modification (Fig. 6*A*–*C*).

Figure 6*G* shows the time course of MTSEA (100 μM) modification of $\alpha1$(T47C)$\beta2\gamma2$ receptors in the control, in the presence of GABA (30 mM) and in the presence of propofol (10 μM). MTSEA in the presence or absence of agonists was applied cumulatively for 500 ms. The time course for modification in each case was well fitted with a single exponential function. The mean ± SEM τ of modification and the extent of functional change are plotted in Figure 6*H* and *I*, respectively. Second-order rate constants are summarized in Table 2. GABA (30 mM) and propofol (10 μM) did not significantly alter the τ of MTSEA modification of $\alpha1$(T47C)$\beta2\gamma2$ receptors. However, both GABA and propofol significantly reduced the extent of MTSEA-mediated inhibition ($P < 0.05$; one-way ANOVA; *post hoc* Tukey's comparison *vs.* control) (Fig. 6*I*).

Discussion

In the present study, we investigated the role of the $\alpha1$ subunit $\beta1$ strand in $GABA_A$ receptor function. Guided by MD simulation data on the SASA of equivalent residues of the $GABA_A$ $\beta3$ homopentamer, we mutated five continuous residues on the $\beta1$ strand of the $GABA_A$ $\alpha1$ subunit to Cys. Whole-cell voltage clamp electrophysiology revealed that D43C, F45C and T47C substitutions caused changes in the GABA concentration–response relationship, demonstrating for the first time that the $\beta1$ strand residues play a role in mammalian pLGIC function.

The $\beta1$ strand runs adjacent and parallel to the critical $\beta2$ strand, which contains loop D. A crucial Phe (Phe64) in the $\beta2$ strand of the $GABA_A$ receptor $\alpha1$ subunit plays a critical role in both GABA binding and the conformational transition that leads to orthosteric gating of the channel (Boileau *et al.* 1999; Szczot *et al.* 2014). These effects also manifest as a large rightward shift in the apparent potency for GABA. The agonist concentration–response relationship (and therefore apparent potencies) are composites of binding and gating events, and both can influence the concentration–response relationship (Colquhoun, 1998). Indeed, $\alpha1$ subunit Phe64 in the $\beta2$ strand, which causes large rightward shifts in the apparent potency of GABA, when Cys-substituted, is an example of a residue with a dual action in binding and gating efficacy (Boileau *et al.* 1999; Szczot *et al.* 2014). Substituted Cys64 in the $GABA_A$ receptor $\alpha1$ subunit was accessible to sulfydryl modification when expressed in *Xenopus* oocytes (Boileau *et al.* 1999; Holden & Czajkowski, 2002). Using fast applications of MTSEA, we showed that the same substitution in $\alpha1\beta2\gamma2$ receptors expressed in HEK-293 cells was modified with a similar second-order rate constant. Furthermore, as noted previously, the presence of GABA slows the rate of Cys64 modification, whereas the allosteric agonist propofol had no effect. This is in contrast to $\alpha1$(D43C)$\beta2\gamma2$ and $\alpha1$(T47C)$\beta2\gamma2$ receptors, where both GABA and propofol affect MTSEA-mediated modification of the substituted Cys, suggesting that $\beta1$ strand residues play a role different from that of Phe64 in the $\beta2$ strand in terms of $GABA_A$ receptor activation.

Changes in Cys accessibility during receptor activation can be a result of either direct or indirect effects of agonists. Direct agonist effects probably arise from

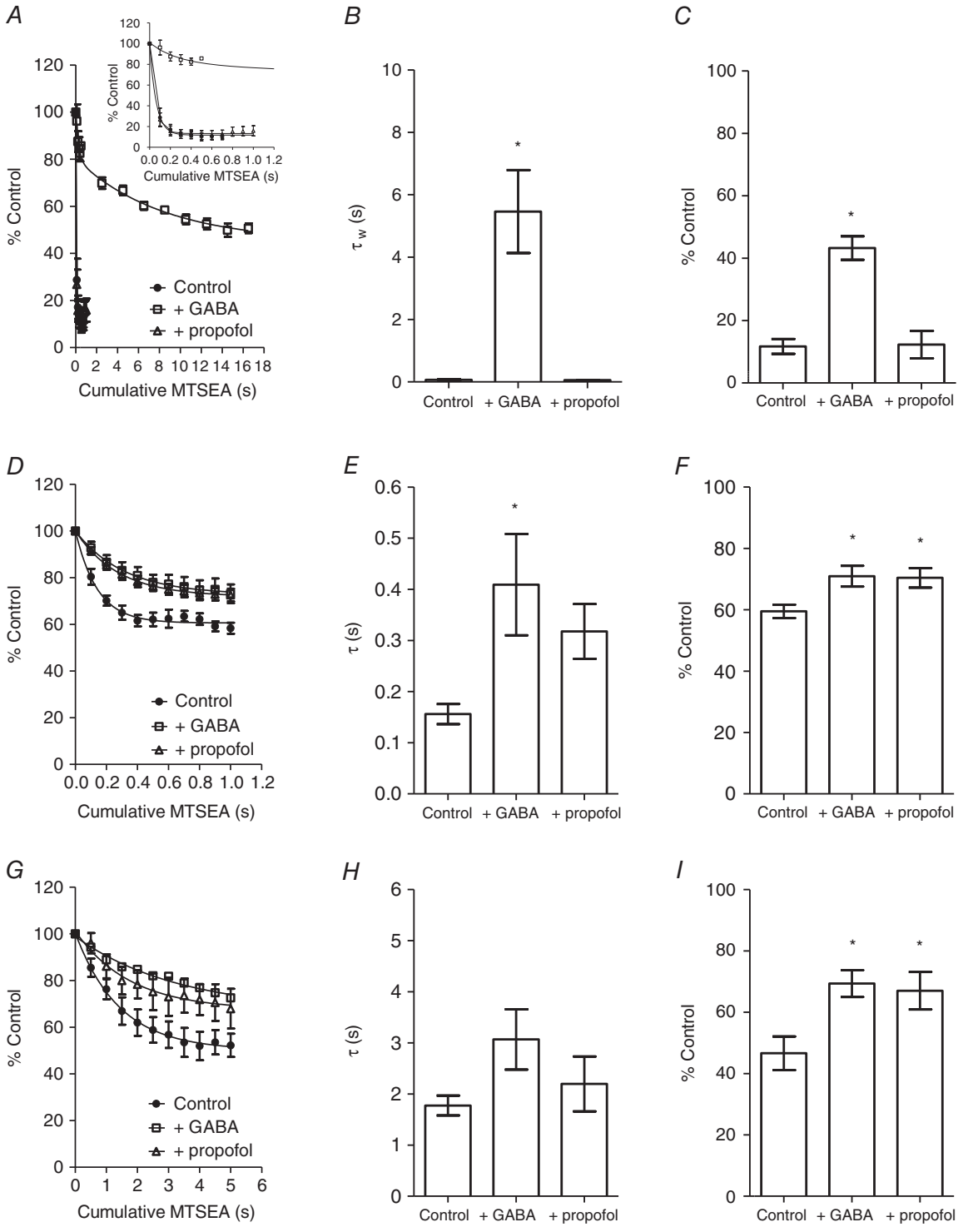

Figure 6. Effect of GABA and propofol on MTSEA modification of Cys-substituted receptors
A, rate of MTSEA (10 μM) modification of α1(F64C)β2γ2 receptors in the control (solid circles) and in the presence of GABA (300 mM; open squares) or propofol (10 μM; open triangles). The line shows the exponential function fitted to the data points. Inset in (*A*) shows, on an expanded time scale, the difference in rate of MTSEA modification in the presence or absence of agonists. *B*, graph showing mean ± SEM τ MTSEA modification of α1(F64C)β2γ2 receptors. The τ of MTSEA modification in control, GABA and propofol was 0.065 ± 0.02 s (n = 4), 5.5 ± 1.3 s (n = 4) and 0.057 ± 0.001 s (n = 5). The presence of GABA significantly increased the τ of MTSEA modification (*P < 0.001; one-way ANOVA; *post hoc* Tukey's comparison). *C*, graph showing mean ± SEM extent of MTSEA

hindrance of the substituted Cys by the bound agonist (protection), whereas indirect effects probably arise from conformational changes induced by the agonist that alter the position of the substituted Cys, making it less accessible. Our data show that an activating concentration of propofol impairs the accessibility of both Cys43 and Cys47 in a manner similar to a maximally effective concentration of GABA. This is consistent with a conformational change associated with gating resulting in reduced accessibility of positions 43 and 47. This also suggests that the structural rearrangements in the β1 strand of the $GABA_A$ receptor α1 subunit are similar, irrespective of agonist binding in the vicinity or far away from the orthosteric binding site. A conformational change in this region makes sense given the anti-parallel location of the β1 relative to the β2 strand, together constituting a hairpin structure that participates in the transduction of binding to $GABA_A$ channel opening. Indeed, Kash *et al.* (2003) implicated an interaction between the loop connecting the β1 and β2 strands of the α1 subunit, and the TM2–3 loop during $GABA_A$ receptor activation. Furthermore, we have previously demonstrated that substitution of the conserved α1 subunit TM2-3 Lys278 with methionine reduces the efficacy of activation by GABA and propofol (Hales *et al.* 2006). The same mutation also reduced the level of spontaneous gating of α1(K278M)β2γ2 $GABA_A$ receptors consistent with a global reduction in gating (Othman *et al.* 2012). Comparison of the open (ivermectin and glutamate bound) and closed (*apo*) structures of GluCl also reveals movement in this region associated with channel opening (Althoff *et al.* 2014). During activation, there is a downward displacement of the β1–β2 loop, increasing its proximity to the TM2–3 loop. The agonist bound and apo-GluCl models also reveal large movements of residues within the β1 and β2 strands, particularly Arg37 in the β1 strand, homologous to Thr47 in the present study. Comparison of the open (glycine bound) and closed (strychnine bound) structures of the zebrafish glycine receptor reveal similar movements of the β1–β2 loop (Du *et al.* 2015). It is therefore becoming evident that residues along the β1 and β2 strands are well positioned to participate in the transduction of agonist binding to gating.

Although α1(D43C)β2γ2 and α1(T47C)β2γ2 receptors were sensitive to MTSEA modification, α1(I42C)β2γ2, α1(F45C)β2γ2 and α1(V46C)β2γ2 receptors were not. The low SASA values of the residues homologous to those in position 42 and 46 of the $GABA_A$ β3 homopentamer (Ile42 and Ile44, respectively) (Fig. 1) suggest that these residues are not solvent exposed but, instead, have their side chains orientated within a hydrophobic environment. However, the homologous position to Cys45 in the $GABA_A$ β3 homopentamer (Asp43) is solvent accessible; this contrasts with our SCAM data, which demonstrate that Cys45 is not modifiable by MTSEA or PhMTS. It is possible that the carboxylate group of Asp43 (equivalent to Phe45 in α1) causes an increased hydration of the agonist binding site in the case of the β3 homopentamer, as it has previously been shown that negatively-charged side chains can promote solvation even in highly hydrophobic regions (Krah *et al.* 2010; Villinger *et al.* 2010). The structure of the α1 subunit within the heteromeric α1β2γ2 receptor may also differ significantly from the β3 subunit, altering the environment of α1 residue 45 relative to the equivalent β3 residue 43. The most obvious structural difference between these two subunits in the vicinity of this residue is in loop F, which, together with loop D, sandwich the β1 strand. Loop F has two fewer residues in the α1 subunit compared to the β3 subunit.

Our data also demonstrate that α1(F45C)β2γ2 receptors have a biphasic GABA concentration–response relationship with increased spontaneous gating. The component of the biphasic GABA concentration–response relationship, with the higher apparent potency, may occur as a consequence of increased spontaneous gating observed for α1(F45C)β2γ2 relative to WT receptors. Our finding that α1(F45C)β2γ2 exhibits increased

modification of α1(F64C)β2γ2 receptors. The extent of MTSEA modification in control, GABA and propofol was 12 ± 2.4% (n = 4), 43 ± 3.8% (n = 4) and 12 ± 4.4 s (n = 5). The presence of GABA significantly reduced the extent of MTSEA modification (*P < 0.0001; one-way ANOVA; *post hoc* Tukey's comparison). *D*, as in (*A*), the rate of MTSEA (100 μM) modification of α1(D43C)β2γ2 receptors. *E*, mean ± SEM τ MTSEA modification of α1(D43C)β2γ2 receptors. The τ of MTSEA modification in control, GABA (300 mM) and propofol (10 μM) was 0.16 ± 0.02 s (n = 6), 0.41 ± 0.10 s (n = 6) and 0.32 ± 0.054 s (n = 7). The presence of GABA significantly increased the τ of MTSEA modification (*P < 0.05; one-way ANOVA; *post hoc* Tukey's comparison). *F*, mean ± SEM extent of MTSEA modification of α1(D43C)β2γ2 receptors. The extent of MTSEA modification in control, GABA and propofol was 60 ± 2.2% (n = 6), 71 ± 3.4% (n = 6) and 70 ± 3.2% (n = 7). The presence of GABA and propofol significantly reduced the extent of MTSEA modification (*P < 0.05; one-way ANOVA; *post hoc* Tukey's comparison). *G*, as in (*A*), the rate of MTSEA (100 μM) modification of α1(T47C)β2γ2 receptors. *H*, mean ± SEM τ MTSEA modification of α1(T47C)β2γ2 receptors. The τ of MTSEA modification in control, GABA (30 mM) and propofol (10 μM) was 1.8 ± 0.19 s (n = 8), 3.1 ± 0.59 s (n = 5) and 2.2 ± 0.54 s (n = 6). There was no significant difference in the τ of modification (P = 0.13; one-way ANOVA). *I*, mean ± SEM extent of MTSEA modification of α1(T47C)β2γ2 receptors. The extent of MTSEA modification in control, GABA and propofol was 47 ± 5.5% (n = 8), 69 ± 4.4% (n = 5) and 67 ± 6.1% (n = 6). The presence of GABA and propofol significantly reduced the extent of MTSEA modification (*P < 0.05; one-way ANOVA; *post hoc* Tukey's comparison).

spontaneous gating suggests that residue Phe45 stabilizes the receptor in the inactive conformation.

Mutations that increase spontaneous gating typically cause a left-shifted concentration–response relationship, where receptors have a higher sensitivity to agonists (Mortensen *et al.* 2003; Hadley & Amin, 2007). The component of the $\alpha1$(F45C)$\beta2\gamma2$ concentration–response relationship, with a lower apparent potency, has a shallow Hill coefficient (~0.5) (Fig. 3*A* and Table 1), suggesting that co-operativity between adjacent GABA binding sites is impaired. It is worth considering how residue 45 in the first occupied orthosteric site may participate in communication with the subsequently occupied binding site. As noted previously, the $\beta1$ strand lies between loop D on the $\beta2$ strand and loop F. Loop F in $GABA_A$ $\rho1$ homopentamers and $\alpha1\beta2\gamma2$ heteromers has been implicated in co-operativity of binding and gating, respectively. Site-directed fluorescence spectroscopy of $GABA_A$ $\rho1$ receptors, implicated structural rearrangements in loop F during orthosteric ligand binding, which were unrelated to gating (Khatri *et al.* 2009). Interestingly, for $GABA_A$ $\rho1$ receptors, a number of loop F Cys substitutions appeared to reduce the Hill coefficient. Loop F residues in the $\gamma2$ subunit are also implicated in transducing benzodiazepine binding events to altered gating (Hanson & Czajkowski, 2008) and it has been postulated that loop F residues play a role in the cooperativity of agonist binding (Khatri & Weiss, 2010). Phe45 in the $\beta1$ strand of the $GABA_A$ $\alpha1$ subunit may transduce structural rearrangements within the binding pocket to the adjacent binding domain, via loop F. Therefore, the lack of Phe45 in the $\alpha1$(F45C)$\beta2\gamma2$ receptor may lead to an uncoupling of binding between the two orthosteric binding sites. In addition, the existence of receptors in either the spontaneously open conformation or in the closed state may provide an explanation for the high and low sensitivity components of the concentration–response relationship.

Residues in the $\beta1$ and $\beta2$ strands of the *Erwinia chrysanthemi* ligand-gated ion channel (Pan *et al.* 2012) and neuronal $\alpha7$ ACh receptors (Quiram *et al.* 2000) have been implicated in the recognition of antagonists. The *C. elegans* GluCl α subunit homopentamer is the only structure that implicates $\beta1$ strand residues in agonist binding and, consequently, this region was postulated to be a seventh ligand-binding loop, termed loop G (Hibbs & Gouaux, 2011). Arg45 in the *C. elegans* GluCl α subunit appears to participate in glutamate binding. By contrast, $\beta1$ strand residues of the $GABA_A$ $\beta3$ (Miller & Aricescu, 2014), as well as the 5-HT_3A receptors (Hassaine *et al.* 2014), lie outside the ligand-binding site. Emerging structural data suggest that a direct role for $\beta1$ strand residues in agonist binding may be restricted to the *C. elegans* GluCl (Blarre *et al.* 2014).

Our findings suggest that naturally occurring mutations and polymorphisms affecting the $\beta1$ strand may result in functional deficits that could be pathological. We are unaware of any such mutations that have been identified to date, although knowledge of the importance of this region of the receptor may prove to be important in future studies.

Refinement of the SCAM for use with rapid solution exchange should enable an investigation of altered accessibility caused by specific states of the receptor induced by agonist activation. We anticipate that this approach will help to bridge the gap between static structural models and real time recordings of electrophysiology. This will help to discriminate between the conformational changes caused by activation and desensitization.

References

Althoff T, Hibbs RE, Banerjee S & Gouaux E (2014). X-ray structures of GluCl in apo states reveal a gating mechanism of Cys-loop receptors. *Nature* **512**, 333–337.

Anandakrishnan R, Aguilar B & Onufriev AV (2012). H++ 3.0: automating pK prediction and the preparation of biomolecular structures for atomistic molecular modelling and simulations. *Nucleic Acids Res* **40**, W537–W541.

Baptista-Hon DT, Deeb TZ, Lambert JJ, Peters JA & Hales TG (2013). The minimum M3-M4 loop length of neurotransmitter-activated pentameric receptors is critical for the structural integrity of cytoplasmic portals. *J Biol Chem* **288**, 21558–21568.

Berger O, Edholm O & Jahnig F (1997). Molecular dynamics simulations of a fluid bilayer of dipalmitoylphosphatidylcholine at full hydration, constant pressure, and constant temperature. *Biophys J* **72**, 2002–2013.

Blarre T, Bertrand HO, Acher FC & Kehoe J (2014). Molecular determinants of agonist selectivity in glutamate-gated chloride channels which likely explain the agonist selectivity of the vertebrate glycine and GABAA-rho receptors. *PLoS ONE* **9**, e108458.

Boileau AJ, Evers AR, Davis AF & Czajkowski C (1999). Mapping the agonist binding site of the GABAA receptor: evidence for a beta-strand. *J Neurosci* **19**, 4847–4854.

Boileau AJ, Newell JG & Czajkowski C (2002). GABA(A) receptor beta 2 Tyr97 and Leu99 line the GABA-binding site. Insights into mechanisms of agonist and antagonist actions. *J Biol Chem* **277**, 2931–2937.

Bussi G, Donadio D & Parrinello M (2007). Canonical sampling through velocity rescaling. *J Chem Phys* **126**, 014101.

Calimet N, Simoes M, Changeux JP, Karplus M, Taly A & Cecchini M (2013). A gating mechanism of pentameric ligand-gated ion channels. *Proc Natl Acad Sci USA* **110**, E3987–E3996.

Colquhoun D (1998). Binding, gating, affinity and efficacy: the interpretation of structure-activity relationships for agonists and of the effects of mutating receptors. *Br J Pharmacol* **125**, 924–947.

Contreras FX, Ernst AM, Wieland F & Brugger B (2011). Specificity of intramembrane protein-lipid interactions. *Cold Spring Harb Perspect Biol* **3**, pii: a004705.

Cromer BA, Morton CJ & Parker MW (2002). Anxiety over GABA(A) receptor structure relieved by AChBP. *Trends Biochem Sci* **27**, 280–287.

Du J, Lu W, Wu S, Cheng Y & Gouaux E (2015). Glycine receptor mechanism elucidated by electron cryo-microscopy. *Nature* **526**, 224–229.

Eisenhaber F, Lijnzaad P, Argos P, Sander C & Scharf M (1995). The double cubic lattice method: efficient approaches to numerical integration of surface area and volume and to dot surface contouring of molecular assemblies. *J Comput Chem* **16**, 12.

Feenstra AK, Hess B & Berendsen Herman JC (1999). Improving efficiency of large time-scale molecular dynamics simulations of hydrogen-rich systems. *J Comput Chem* **20**, 13.

Goldschen-Ohm MP, Wagner DA & Jones MV (2011). Three arginines in the GABAA receptor binding pocket have distinct roles in the formation and stability of agonist- versus antagonist-bound complexes. *Mol Pharmacol* **80**, 647–656.

Hadley SH & Amin J (2007). Rat alpha6beta2delta GABAA receptors exhibit two distinct and separable agonist affinities. *J Physiol* **581**, 1001–1018.

Hales TG, Deeb TZ, Tang H, Bollan KA, King DP, Johnson SJ & Connolly CN (2006). An asymmetric contribution to gamma-aminobutyric type A receptor function of a conserved lysine within TM2-3 of alpha1, beta2, and gamma2 subunits. *J Biol Chem* **281**, 17034–17043.

Hanson SM & Czajkowski C (2008). Structural mechanisms underlying benzodiazepine modulation of the GABA(A) receptor. *J Neurosci* **28**, 3490–3499.

Hassaine G, Deluz C, Grasso L, Wyss R, Tol MB, Hovius R, Graff A, Stahlberg H, Tomizaki T, Desmyter A, Moreau C, Li XD, Poitevin F, Vogel H & Nury H (2014). X-ray structure of the mouse serotonin 5-HT3 receptor. *Nature* **512**, 276–281.

Heckman KL & Pease LR (2007). Gene splicing and mutagenesis by PCR-driven overlap extension. *Nat Protoc* **2**, 924–932.

Hess B, Bekker H, Berendsen HJC & Fraaije JGEM (1997). LINCS: A linear constraint solver for molecular simulations. *J Comput Chem* **18**, 10.

Hibbs RE & Gouaux E (2011). Principles of activation and permeation in an anion-selective Cys-loop receptor. *Nature* **474**, 54–60.

Holden JH & Czajkowski C (2002). Different residues in the GABA(A) receptor alpha 1T60-alpha 1K70 region mediate GABA and SR-95531 actions. *J Biol Chem* **277**, 18785–18792.

Hornak V, Abel R, Okur A, Strockbine B, Roitberg A & Simmerling C (2006). Comparison of multiple Amber force fields and development of improved protein backbone parameters. *Proteins* **65**, 712–725.

Humphrey W, Dalke A & Schulten K (1996). VMD: visual molecular dynamics. *J Mol Grap* **14**, 33–38, 27–38.

Kash TL, Jenkins A, Kelley JC, Trudell JR & Harrison NL (2003). Coupling of agonist binding to channel gating in the GABA(A) receptor. *Nature* **421**, 272–275.

Khatri A, Sedelnikova A & Weiss DS (2009). Structural rearrangements in loop F of the GABA receptor signal ligand binding, not channel activation. *Biophys J* **96**, 45–55.

Khatri A & Weiss DS (2010). The role of Loop F in the activation of the GABA receptor. *J Physiol* **588**, 59–66.

Krah A, Pogoryelov D, Meier T & Faraldo-Gomez JD (2010). On the structure of the proton-binding site in the F(o) rotor of chloroplast ATP synthases. *J Mol Biol* **395**, 20–27.

Lindorff-Larsen K, Piana S, Palmo K, Maragakis P, Klepeis JL, Dror RO & Shaw DE (2010). Improved side-chain torsion potentials for the Amber ff99SB protein force field. *Proteins* **78**, 1950–1958.

Miller PS & Aricescu AR (2014). Crystal structure of a human GABA receptor. *Nature*.

Mortensen M, Wafford KA, Wingrove P & Ebert B (2003). Pharmacology of GABA(A) receptors exhibiting different levels of spontaneous activity. *Eur J Pharmacol* **476**, 17–24.

Newell JG & Czajkowski C (2003). The GABAA receptor alpha 1 subunit Pro174-Asp191 segment is involved in GABA binding and channel gating. *J Biol Chem* **278**, 13166–13172.

Othman NA, Gallacher M, Deeb TZ, Baptista-Hon DT, Perry DC & Hales TG (2012). Influences on blockade by t-butylbicyclo-phosphoro-thionate of $GABA_A$ receptor spontaneous gating, agonist activation and desensitization. *J Physiol* **590**, 163–178.

Pan J, Chen Q, Willenbring D, Yoshida K, Tillman T, Kashlan OB, Cohen A, Kong XP, Xu Y & Tang P (2012). Structure of the pentameric ligand-gated ion channel ELIC cocrystallized with its competitive antagonist acetylcholine. *Nat Commun* **3**, 714.

Paramo T, East A, Garzon D, Ulmschneider MB & Bond PJ (2014). Efficient characterization of protein cavities within molecular simulation trajectories: trj_cavity. *J Chem Theory Comp* **10**, 2151–2164.

Parrinello M & Rahman A (1981). Polymorphic transitions in single-crystals – a new molecular-dynamics method. *J Appl Phys* **52**, 9.

Pronk S, Pall S, Schulz R, Larsson P, Bjelkmar P, Apostolov R, Shirts MR, Smith JC, Kasson PM, van der Spoel D, Hess B & Lindahl E (2013). GROMACS 4.5: a high-throughput and highly parallel open source molecular simulation toolkit. *Bioinformatics* **29**, 845–854.

Quiram PA, McIntosh JM & Sine SM (2000). Pairwise interactions between neuronal alpha(7) acetylcholine receptors and alpha-conotoxin PnIB. *J Biol Chem* **275**, 4889–4896.

Schmidt TH & Kandt C (2012). LAMBADA and InflateGRO2: efficient membrane alignment and insertion of membrane proteins for molecular dynamics simulations. *J Chem Inf Model* **52**, 2657–2669.

Smith GB & Olsen RW (1995). Functional domains of GABAA receptors. *Trends Pharmacol Sci* **16**, 162–168.

Szczot M, Kisiel M, Czyzewska MM & Mozrzymas JW (2014). alpha1F64 Residue at GABA(A) receptor binding site is involved in gating by influencing the receptor flipping transitions. *J Neurosci* **34**, 3193–3209.

Tran PN, Laha KT & Wagner DA (2011). A tight coupling between beta(2)Y97 and beta(2)F200 of the GABA(A) receptor mediates GABA binding. *J Neurochem* **119**, 283–293.

Venkatachalan SP & Czajkowski C (2008). A conserved salt bridge critical for GABA(A) receptor function and loop C dynamics. *Proc Natl Acad Sci USA* **105**, 13604–13609.

Villinger S, Briones R, Giller K, Zachariae U, Lange A, de Groot BL, Griesinger C, Becker S & Zweckstetter M (2010). Functional dynamics in the voltage-dependent anion channel. *Proc Natl Acad Sci USA* **107**, 22546–22551.

Wagner DA, Czajkowski C & Jones MV (2004). An arginine involved in GABA binding and unbinding but not gating of the GABA(A) receptor. *J Neurosci* **24**, 2733–2741.

Whiting PJ, McKernan RM & Wafford KA (1995). Structure and pharmacology of vertebrate GABAA receptor subtypes. *Int Rev Neurobiol* **38**, 95–138.

Additional information

Competing interests

The authors declare that they have no competing interests.

Author contributions

DTB-H, UZ and TGH designed the work. DTB-H and AK acquired the data. DTB-H, AK, UZ and TGH analysed and interpreted the data. DTB-H, AK, UZ and TGH drafted the work and revised it critically for intellectual content. All authors approved the final version of this manuscript and agree to be accountable for all aspects of the work in ensuring that questions relating to the accuracy and integrity of the work are appropriately investigated and resolved. All authors qualify for authorship and only those who qualify for authorship are listed.

Funding

The authors would like to thank Tenovus Scotland and Scottish Universities' Physics Alliance (SUPA) for funding.